Rubidium isotope shift measurement made simple

A. Anderson,[*] T. Ayers,[†] S. Cart,[‡] V. Correa-Tobar,[§]
A. O'Brien,[¶] R. Stipanovich,[**] and M. Crescimanno[††]
Department of Physics and Astronomy,
Youngstown State University, Youngstown, OH, 44555

(Dated: October 20, 2025)

Abstract

Experimentally determining the isotope shift leads students beyond their naive understanding of atomic structure and can introduce them to the basics of optical metrology. Earlier undergraduate laboratory experiments for the isotope shift on the principal D1 and D2 transitions in Rubidium typically relied on saturated absorption spectroscopy. We show that using a different atomic state, namely the $5D^{5/2}$ level significantly simplifies the data collection, analysis and interpretation all the while yielding a measurement within a percent of the accepted value. Using nothing more than free-running laser diodes, a cell, a few low-bandwidth photodiodes and a Fabry-Perot cavity this laboratory experience forces students to recognize the necessity of a third (beyond the effect of the nucleus's countermotion and the finite nuclear charge radius) contribution of the isotope shift, the specific mass shift (SMS).

I. INTRODUCTION:

The pedagogic value of doing an isotope shift laboratory is that it refines and expounds upon the atomic physics lessons that the students learn as part of their junior/senior physics sequence. Asking undergraduate physics majors about their 'picture' of the atom often reveals common misconceptions, among them the notion that the nucleus 'sits' at the center of a symmetrical electron cloud. If so, then why would the mass of the nucleus itself play any role in the electronic excitation spectrum? Of course, an appeal to their classical understanding reveals that the nucleus/atomic core must indeed be in countermotion to the electron, which in the S-state is continually moving radially; a laboratory experience measuring the isotope shift reinforces this 'picture' of co-motion inside the atom, but also goes beyond it. Isotope shift measurements in the optical section of the undergraduate advanced laboratory appears to have traditionally been done by comparing the hydrogen and deuterium Balmer series using a monochromator and a photomultiplier tube (PMT) **??** though relatively low cost, compact, medium resolution spectrometer also suffice. Doing so one recovers the aforementioned effect of the nuclear orbital co-motion without being sensitive to the much smaller isotope nuclear size effects. In contrast, experiments using rubidium's brightest transitions at 780nm (D2) and 795nm (D1) contain both the effect of the core's countermotion and the nuclear size effects as well as a third contribution called the specific mass shift (SMS) that is a more subtle consequence of the perturbations on the multi-electron wavefuntion for that state.

We present a greatly simplified approach to the isotope shift measurement by using a free-running 776nm laser in conjunction with a 780nm laser to excited and study the shift in a 2-photon excited state, the $5D^{\frac{5}{2}}$ state. The spectral compactness of the hyperfine states of the $5D^{\frac{5}{2}}$ makes the data analysis much simpler for the students, and allows one to experimentally unambigiously distinguish the SMS contribution. The approach we describe here is simple in that it uses only standard laboratory-grade photodiode detectors (no PMT) and COTS optics.

In practice this leads to a determination of the isotope shift that is within a MHz of the value known from precision experiment, and is therefore inherently more accurate than the common approach based on Saturated Absorption Spectroscopy[2] (SAS). In the approach detailed below, since a higher excited state is used, the hyperfine splittings of that state are

so small that one may approximate the entire optical response as if it were a single state; it is as if the lineshape already comprises the excited state weighted sum (as in Eq.4 for the ground state) needed in computing the isotope shift.

Laser diodes have long been used in hyperfine spectroscopy on both of the principal near infrared optical transitions (called the "D1" at 795nm or "D2" at 780nm respectively, see Fig.1 and Fig.3, green line). The use of SAS technique on these transitions in measuring the isotope shift forms extensive existing literature typically employing Extended Cavity Diode Lasers (ECDLs)[4,5], or somewhat more intricate cavity stabilized schemes.[6,7] For more details on the physics of the laser diode and the historical development of their use in atomic spectroscopy see Ref.[8]. There is significant literature on SAS's use in higher excited state levels, notably[4,9–12], and even pulsed lasers , for example in Ref.[6,13], as well as for other atomic species[14], even with free-running (non ECDL) laser diodes.[15] Quantifying the isotope effect on the 780nm (D2)/795nm (D1) fine structure split transitons in Rubidium also has a celebrated history[16,23–27] (read Ref.[28] for a more up-to-date experimental summary of isotope shift measurements specific to rubidium), and more recently precision measurements of the isotope shift have been of interest for the indirect detection of new physical interactions[29–31].

Measuring the isotope shift using higher excited states via two-photon transitions in Rubidium hails from the mid 1970's[16,17]. These early measurements were meant primarily as surveys and had uncertainties that were large by modern standards (and also in comparison with the approach here). A much more accurate measurement of the isotope shift through the use of a rather elaborate microwave standard referenced frequency chain was first possible in the 1990's, which reported the isotope shift for the state of interest for the current paper, the $5D_{\frac{5}{2}}^{5}$ state in Rubidium, of 163.033 (6) MHz[18]. That team was able to use their setup to measure a whole host of shifts in different levels and different atomic species, with about the same accuracy. The advent and diffusion of frequency combs has significantly extended the precision of other efforts to measure isotope shifts, including in the 6P levels of Rubidium[19]. Turnkey frequency combs systems are still rather expensive and their use in this application requires heterodyne detection and signal recovery technique beyond that typically required for an undergraduate advanced laboratory.

Over the last 20+ years much of the laser diode spectroscopy technique has become part of the cannon of the advanced undergraduate laboratory.[38] Of particular interest beyond measuring the isotope shift, laser diode spectroscopy has been used to teach about Doppler

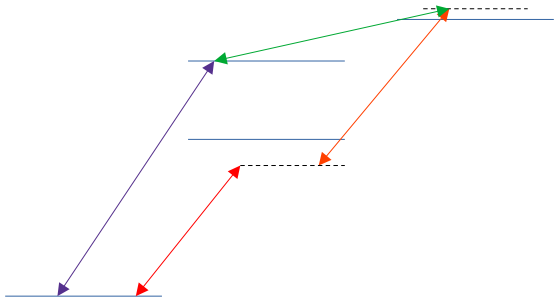

FIG. 1. The level sructure and laser transitions used in this work. This paper describes an elementary laboratory for measuring the ground state isotope shift. Not all atomic levels are shown.

broadening[39] , radiative broadening[40], non-linear spectroscopy[41], noise spectroscopy[42], SAS lineshape[43,44].

This experiment uses commodity Indium Gallium Arsenide near infrared laser diodes for which the emission wavelength (∼780nm) varies smoothly with temperature and current over limited ranges, puncuated by large abrupt changes called "mode hops". Mode hops arise from the temperature-induced relative change of the laser diode's Fabry-Perot resonances relative to the intrinsic gain envelope of the semiconductor. These hops not withstanding, we have found that about a fourth of the 780nm diodes we have cooled with a thermoelectric coolers (TEC) are tunable onto 776nm 5P-5D transition in Rubidium. For our use here, an admittedly crude temperature stabilization suffices, allowing those interested in implementing this laboratory to avoid the additional cost and optical/mechanical complexity associated with making these 776nm sources into ECDLs.

Comparing a pair (or more) of transitions on a pair of isotopes one can determine the three distinct contributions to the isotopic difference: (1) the naive mass shift (from the nuclear countermotion of the excited atomic core about the center of mass of the unexcited atom),

(2) the nuclear "field shift" (due to the spatial structure of the charge density in the nucleus) and (3) the so-called specific mass shift (SMS). The first two contributions are rather easy to conceptualize and determine using the D1 (795nm) and D2 (780nm) in SAS[2]. However with those measurements one cannot easily disentangle the SMS contribution as a distinct contribution. The SMS contribution is somewhat harder for students to conceptualize. It is a consequence of changes in the many-body electronic kinetic energy in going from one isotope to another, and so is intrinsically a (many body-)wavefunction effect. For some recent examples of experimental accounting for these contributions see Ref.[20] for Neon and Ref.[21] for excited states of atomic Titanium. A very readable and concise theoretical synopsis of the calculation of the effect can be found in[3]. One advantage of measuring the isotope shift via a second excited state, such as the $5D^{5/2}$ as presented here, is that it leads students rather directly to an estimate of the SMS as a distinct contribution.

We have already mentioned that, at the complexity "cost" of making and tuning the 776nm laser, the resulting interpretation and computation of the associated isotope shift is simpler than for the 5P levels. Note also that the earlier 5P level SAS version of this lab one had a systematic error from the visibility of unresolved 5P hyperfine states. These contributions are ignored in computing the "center of mass" of the excited state manifolds (those '...' in the above) due to their generally poor visibility. In Ref.[2] here it was noted that if one includes as a naive estimate for these "missing" transitions ^{85}Rb F=3 $\rightarrow$ F'=1 and the ^{87}Rb F=2 $\rightarrow$ F'=0 as being as far in energy from their neighbor (the ^{85}Rb F=3 $\rightarrow$ F'=2 and the ^{87}Rb F=2 $\rightarrow$ F'=1) as those states are in turn from their respective neighbors (the ^{85}Rb F=3 $\rightarrow$ F'=3 and the ^{87}Rb F=2 $\rightarrow$ F'=2), one finds an isotope shift of 79 MHz (resulting in a ground state energy shift of 172 MHz), somewhat closer to the accepted value.

Because the hyperfine intervals for the 5D level accessed by the 776nm laser are so much smaller than those of the 5P one need not account for the individual state-averaged hyperfine state locations. Instead, in the experiment it suffices to identify a single composite transition for the 5D level of each isotope, the excited state hyperfine components overlapping. Although that sounds like a disadvantage it greatly simplifies the student computation, and by going to the next order of analysis and quantifying the lineshape distortion associated with these overlapping excited state hyperfine components, show why ignoring this excited hyperfine sub-structure of the transition for the 5D works as well as it does.

REPEAT? FIX! The additional complexity of using rubidium isotopes as compared with

the spectral comparison between those of hydrogen is that for rubidium isotopes one must include the hyperfine splittings of both the ground state and excited states in the analysis. Fortunately this is simple and straightforward to do, since the hyperfine level splittings are parameterized via[24,25]. By using the $5D^{5/2}$ level, the electron on average being so much further away from the nucleus, the hyperfine splittings are correspondingly much smaller, and are expected to about that of the free running 776nm laser linewidth itself.

II. THEORY:

In its simplest form, the isotope shifts in an elemental spectrum are the result of the nuclear countermotion, the nuclear charge distribution and changes in the many-body electronic contribution to the kinetic energy. (see Ref.[47] for a student-friendly, very readable and comprehensive current theory review of isotope shifts in complex atoms). Students will be familiar with the fact that the energy levels of the hydrogen atom are proportional to the reduced mass $\mu = mM/(m + M)$ where m is the electron mass and M is the nuclear mass. Rubidium, being hydrogen-like (in having a mostly isolated single electron in its outmost shell) then is expected to also , to leading order, have energies proportional to μ. This μ-scaling of the first term in the energy in literature is referred to as "the normal mass shift" , or NMS. Of course, that formula assumes that all the charge is at $r = 0$, whereas the nuclear charge is effectively spread out over roughly a fermi. This causes a deviation from a pure Coulomb potential that also perturbs the state energies, primarily of the S-wave electronic states which have "pentration at the nucleus" and so can – in pertubation theory – 'see' this deviation. This non-nuclear mass related effect is called the "nuclear shift" or NS contributions. This effect is sometimes referred in the literature as the "field effect" term.

The third distinct contribution, called the "Specific Mass Shift" or SMS is from secondary differences in the multielectron wavefunction between isotopes. These arise from the multielectron kinetic term changing slightly between isotopes. Unlike the other two contributions (NMS and NS), the SMS is harder to conceptualize, being a consequence of the effect that the wavefunction change from the NS, filtered through the Fermi symmetry of the full many-body wavefunction, has on the kinetic terms.

To illustrate the SMS contribution to the isotope effect consider a 3 body quantum

mechanics problem involving one nucleus and a pair of identical fermions. We regard the fermions as 'spinless' in that we require full antisymmetrization under exchange but do not include any internal contribution to the wavefunction. The Hamiltonian reads

$$H = \frac{P^2}{2M} + \frac{p_1^2}{2m} + \frac{p_2^2}{2m} + V(R - r_1) + V(R - r_2) + V_f(r_1 - r_2) \tag{1}$$

where P (p_i , $i = 1, 2$) is the momentum of the nucleus , mass M (fermions mass m, respectively). In separating the center of mass motion out from the relative motions, one finds a re-organization of the quadratic terms:

$$H = H_{cm} + \frac{M^2}{(M+2m)^2}\big[\frac{\pi_1^2}{2\mu} + \frac{\pi_2^2}{2\mu} + \frac{\pi_1\pi_2}{M}\big] + V(x_1) + V(x_2) + V_f(x_1 - x_2) \tag{2}$$

where π_i is conjugate to the relative co-ordinates x_i, and μ is the single particle reduced mass $mM/(M+m)$. The $\frac{\pi_1\pi_2}{M}$ is the SMS term that leads to a shift beyond the nuclear and normal isotope shifts discussed earlier. To illustrate the effect of the SMS term, we now truncate to a Hilbert space spanned by tensor products of three single-particle states $|a\rangle$, $|b\rangle$ and $|c\rangle$ and evaluate the non-center of mass part of Eq.2. For example, in this single particle basis that the momentum operator π and the nuclear potential V (we for simplicity neglect V_f throughout)

$$\pi = \begin{bmatrix} 0 & \alpha & 0 \\ \alpha^* & 0 & \beta \\ 0 & \beta^* & 0 \end{bmatrix} \qquad V = \begin{bmatrix} V_1 & 0 & -\alpha^*\beta^* \\ 0 & V_2 & 0 \\ -\alpha\beta & 0 & 0 \end{bmatrix} \tag{3}$$

With this choice one sees that the Hamiltonian has an eigenstate $\psi = \frac{1}{\sqrt{2}}(|a\rangle\,|b\rangle - |b\rangle\,|a\rangle)$ of energy *Evaluate*. On the other hand, the single particle contributions to this energy are *singleenergy* so that the difference is the SMS contribution. It is clear that it depends non-trivially on the mass of the nucleus.

Up to this point our discussion did not explicitly include the effects due to the (relative) orientations of the electron spin and magnetic moment of the isotope's nucleus, i.e. hyperfine effects on the spectrum. Assuming an isotropic environment, these result in line splitting and differential line intensity organized only by the total angular momentum quantum number $F = I + j + S$. One can then average out these magnetic splittings completely by forming linear combination of the energies, $E_{0HFS\ ^{85}Rb} = (7dE_+ + 5dE_-)/12$ for ^{85}Rb and $E_{0HFS\ ^{87}Rb} = (5dE_+ + 3dE_-)/8$ for ^{87}Rb as dictated by the I of 5/2 and 3/2 respectively

of the nuclei. These so-called 'center of mass' energies represent the energy of the atomic state were the electron spinless (i.e non-magnetic). These 'synthetic' hyperfine interaction-independent energy levels that result from this multiplicity-weighted averaging are then compared between isotopes to compute the isotope shift.

III. EXPERIMENT:

Although the resulting simplicity of the dataset and its interpretation make this laboratory an attractive addition to or substitute for an isotope shift measurement laboratory, perhaps the biggest hurdle to its widespread implementation is the creation and tuning of the 776nm diode laser source. It is actually not too challenging to build a 776nm diode candidate laser starting from almost any diode that at room temperature is right around 780nm. We use the qualifier "candidate" because in our experience not every diode can function reliably at that wavelength and even if it does, it may 'mode hop' over the wavelengths of spectroscopic interest. We have found in practice that one out of about every three or four diodes can be brought into resonance with the 776nm $5P^{3/2} \rightarrow 5D^{5/2}$ transition in Rubidium.

The diode was mounted in a drilled hole in a thin (2mm thick) aluminum 'T'. On one of the flanges a small outcoupling mirror was mounted (at 45 degrees to the flange). On the stem of the "T" next to the diode a small divot was drilled into the aluminum into which an 10KΩ excapsulated NTC thermistor (a NCP15XH103F03RC negative temperature coefficient thermistor) was afixed. The 'T' is then inverted, and first loosely held in place with a thin thermal paste to a 2mm thich aluminum plate that matched the dimensions of a the face of a $<$ 8amp TEC. The whole plate is then affixed to the TEC with thermal paste, and the other side of the TEC is also pasted and mated with an expanded aluminum heatsink. A mounting hole for holding the assembly is made in the heat sink and the multilayer "sandwich" with the diode and thermistor and mirror in the inverted "T", TEC and heatsink is fastened together with thermally non-conducting restraint band (nylon zipties suffice) and then housed in a styrofoam cover, mostly to limit infiltration of warm air. A thin pellicle of glass can be mounted above the outcoupling mirror to further limit infiltration or air, though often that is not necessary.

A low resolution spectrometer is used to help determine a crude temperature set point

for the control loop to keep the laser near 776nm. For simplicity we chose to use a simple program (link at?) for an Arduino Uno for temperature control. It uses an analog input pin on the Arduino to read the divided voltage from a single 10KΩ resistor in series with the laser package's thermistor is driven by the rather poorly regulated 5V output from the Arduino. The voltge reading is used to to set the pulse-width modulated (PWM) duty cycle it sends to the gate of a single mosfet in series with the TEC and a DC supply (12V). Clearly there are many options to improve on this sufficient but bare-bones laser diode temperature control, but parsimony of parts and ease of modification are its strength.

Once the Arduino-based laser temperature controller is tuned via code, a few minute warm up is all that is needed to get the lab ready for the students. Then, from the student point of view, this lab looks rather straightforward in that the most challenging alignment task is overlapping the counterpropagating beams in the vapor cell (A natural abundance vacuum cell (10cm length and 2.5cm diameter, unshielded and at between 45-80^{o}C) and the adjustment/alignment of the Fabry-Perot (FP) cavity. In the most basic implementation of this laboratory all the data can be readily taken with two slow-speed (0.3mm-square, amplified 5MHz bandwidth) photodetectors hooked to a 2-channel scope (though we found it convenient to use a 4-channel Siglent SDS1204X-E).

First, during a slow (10-100 Hz) current sweep of the 780nm laser, one photodetector receives the 780nm absorption signal from the SAS cell setting the sweep parameters based on the known frequency interval between the SAS resonances in 85Rb. The second photodetector reads the transmission of the FP cavity. We used a relatively low finesse ($\sim$150) confocal 20cm aluminum-body FP cavity not in a temperature regulated enclosure (FP made by Teachspin). Based on these data the free spectral range (FSR) of the FP cavity was measured to be 394$\pm$2 MHz in our experiment. In our implementation the 780nm beam had a total power of 1.4 mW and a diameter at the cell of 1.5mm at the cell window while the 776nm beam had a total power of 0.4mW and a much smaller diameter, $<$ 0.5mm in the cell. We note that the spatial structure of the 780nm beam was much better than the 776nm laser and a 0.75m focal length convex lens upstream from the cell was used to collimate the 776nm down to the reported size in the cell.

Secondly, the photodetector that was collecting the SAS signal is moved to measure the transmission of the 776nm beam during the 780nm sweep. Both lasers are driven with commercial stable current supplies. The 776nm laser current was driven by a Thorlabs

LDC500 and was not swept. The drift rate of the 776nm laser in the thermal enclosure regulated by the Arduino code with this current drive was less than 5MHz/s, as we directly verify in the dataset below. It may be useful to AC couple the photodetector measuring the transmission of the 776nm beam. The 780nm laser was swept (triangle wave), and visually checking the regularity of its FP data indicates that the laser's frequency scan is likely to be free of frequency mode hops. Although the 780nm laser we used was a commercial ECDL, we had no need to modulate the grating peizo, as current modulation was sufficient to span the 10 GHz frequency range without modehops. Being particularly sensitive to back-reflection, we found that a linear polarizer followed by a quarterwave plate upstream was a sufficient reflection isolator to stabilize the 780nm laser from the rest of the experiment during the sweeps. A different waveplate in a rotary mount was plaed upstream of the experiment on the 776nm beam, not for isolation, but to adjust and optimize the signal (absorption changes). Little attention was paid to the polarization dependence of the signal since the changes from polarization choices did not seem so pronounced. All the signal traces are taken quite slowly, and no cable termination was necessary. A triangle wave of sufficient

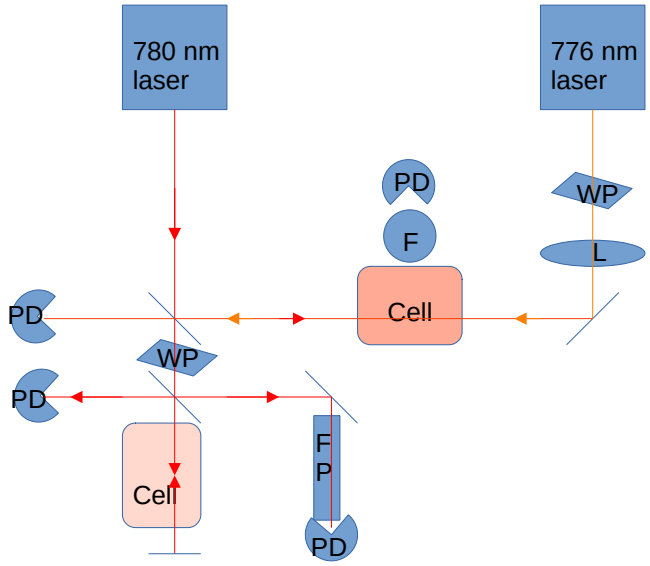

FIG. 2. Experimental Setup: Rb rubidium vapor cell, FP Fabry-Perot cavity, PD photodiodes, BS non-polarizing beam splitter, WP waveplate, F 420nm notch filter (optional), L lens

amplitude was used to modulate the 780nm diode so that its mod-hop free frequency change

spanned the ground state hyperfine states of ^{87}Rb. The 780nm pump and 776nm probe beam paths are then adjusted to overlap inside the vapor cell. Then during the 780nm sweep four distinct 776nm absorption peaks appear, one for each ground state hyperfine level (F=2,3 for 85Rb surounded by F=1,2 of 87Rb) as in Fig. 3. The reason there are only 4 is that the hyperfine splitting in the $5D^{5/2}$ manifold (10's of MHz) is much smaller than the hyperfine splitting in the $5P^{3/2}$ manifold (typically 100MHz) combined with the fact that the free-running 776nm laser's bandwidth is probably in the multi-MHz range. This indicates that the 776nm laser's propagation through the vapor when in resonance cannot resolve the individual hyperfine components of the $5D^{5/2}$ state whereas, in this counter-propagating configuration, it is spectrally pure enough to only connect a single $5P^{3/2}$ hyperfine state with the $5D^{5/2}$ states. Furthermore, since the two lasers are so close in frequency, the doppler offset on the two-photon resonance can be neglected, being essentially the same for each resonance. Such an offset shifts the overall four distinct peaks but cancels out of the isotope shift measurement, significantly simplifying the analysis. On the other hand, a linear drift in the 776nm laser's frequency during the trace would lead to a systematic error in the isotope shift. In practice this can greatly reduced by care in tuning the control loop for the temperature of the diode and increasing the sweep rate. A constant drift rate can be removed entirely by averaging the isotope shift computed during the up-chirp with that of the down-chirp. Although this experiment can be done with a two-channel oscilloscope and pair of photodetectors we opted to use three detectors and a 4-channel oscilloscope to actually measure and bound the 776nm laser's frequency drift effect on the isotope shift measurement. Experimentally achieving 776nm laser frequency drift rates of a few MHz/s was not difficult with the simple Arduino Uno control loop.

The traces are stored digitally and subsequently analyzed by filling out a table of the temporal locations of each FP transmission resonance and the center of each absorption feature (which were fit by gaussians). Best practice for assigning an (offset) frequency to each absorption feature, as described throughout the literature, is not to fit the FP data for a single function of frequency versus sweep time, but instead to simply count whole FSR's (FP resonances) up to the absorption feature and then interpolate across the nearest neighbor FP resonances to the feature's center.

With these measured offset frequencies and their error one can now assemble the isotope shift for this state by taking the difference between the "centers of mass" of the spectra of

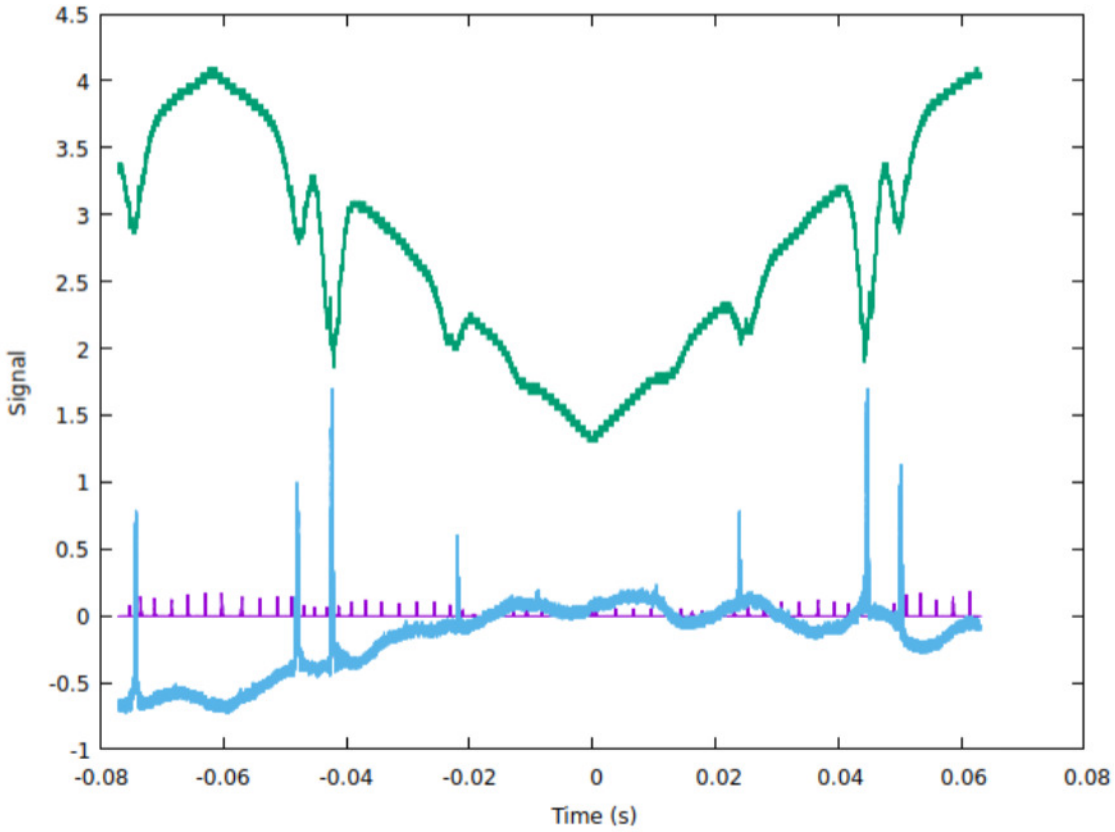

FIG. 3. Typical Oscilloscope traces while 776nm laser (its tranmission in blue) is held fixed and the 780nm laser is swept (its absorption in green). The purple trace is the output of the Fabry-Perot cavity illuminated by a portion of the 780nm laser field.

each isotope, as described in the earlier theory section,

$$\text{Isotope Shift} = (5f_{87Rb\ F=2} + 3f_{87Rb\ F=1})/8 - (7f_{87Rb\ F=3} + 5f_{87Rb\ F=2})/12 \qquad (4)$$

yielding for a set of 10 runs shown in Fig.4 an isotope shift for this state of about 163±1 MHz.

Many versions of this experiment use a 420nm filter coupled with a photomultiplier tube (PMT) to directly measure the flourescence from the $6S^{3/2}$ state in the decay chain of the $5D^{5/2}$. We note that the experiment we report on here made no use of a PMT, but instead a slow amplified photodector behind a 420nm notch filter sufficed to record the flourescence, even at these low powers. The human eye also works well in this regard, as the students enjoyed seeing the blue trace through the notch filter, even recording it on their cell phones during a sweep.

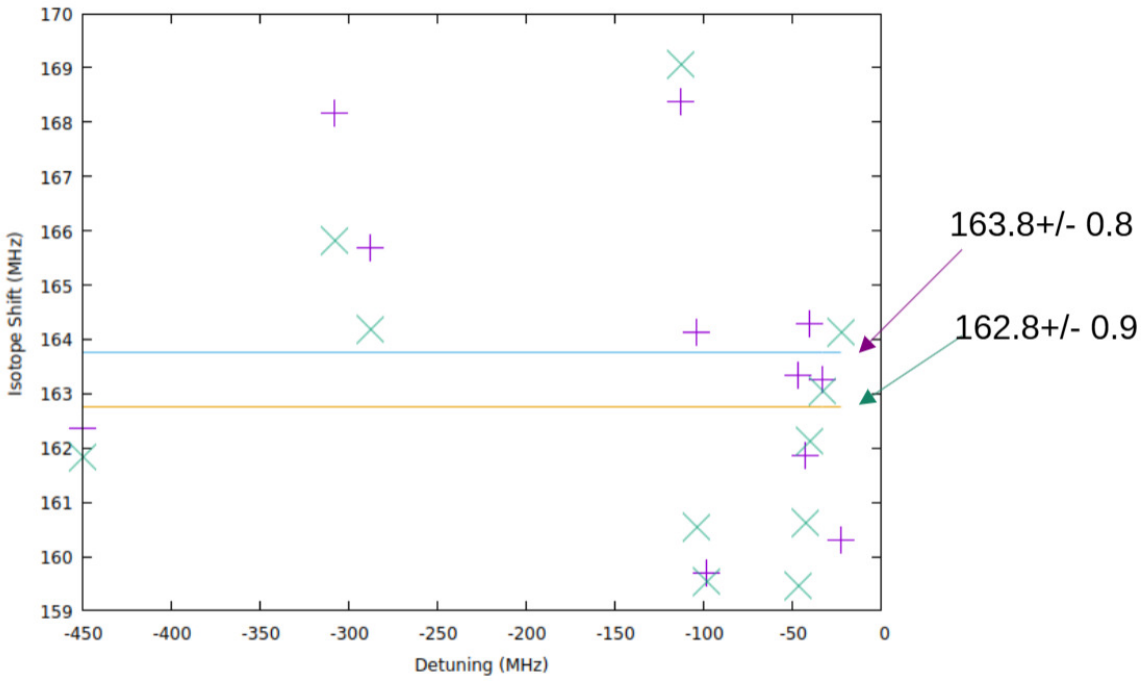

FIG. 4. The measured isotope shift of the 5D5/2 state between ^{87}Rb and ^{85}Rb as a function of the 776nm detuning as described in the text. The green 'x' are using the centers from the full gaussian fit of the FP resonances, whereas the "+" are the result of using just the FP resonance maxima. The gold line is the average using the 'x' data and the blue line is the average using the '+' points.

IV. ANALYSIS AND STUDENT EXPERIENCE

Example of a calculation...brief to get to 164MHz (compare Ref.[]).

The normal mass shift (NMS) alone for this transition (780.25nm photon's f= 3.84 x 10^{14} Hz) is found by μ-scaling, using $df/f = |d\lambda/\lambda|$ leading to df = 57.13 MHz. That means that the 84-57 = 27 MHz is apparently the "nuclear" part (NS) of the isotope shift between ^{85}Rb and ^{87}Rb. The best fit value for this in the literature is about 20 MHz[28].

Now assuming that whole NS part is due to the ground S state (since those electrons spend so much more time than non-S electrons inside the nucleus) only, we can recast the measured isotope shift into a ground state energy difference between the isotopes, relative to the continuum. part of the overall electron binding energy scales with μ, so that one can expect the ratio of the normal part of the isotope shift (NS) to the isotope energy difference be the same as the ratio of the optical excitation energy to the known ionization energy of Rb (4.177 eV). Thus using the fact that our D2 transition at 780.25 nm has an energy of

1.59 eV, we get 57.13(4.177/1.59)+27 = 177 MHz as the ground state energy shift between ^{85}Rb and ^{87}Rb relative to the continuum, and scale this to the $5D^{5/2}$ level.

Then compare with the D1, D2 isotope shift [28,32,34]). Show the SMS that is needed to cohere these results.

V. MODULATION TRANSFER SPECTROSCOPY USE LASER/ATOM LINESHAPE MEASUREMENT

Because it is a two-beam non-linear optical process, the multi-photon process here lends itself to a simple, student-friendly demonstration of the utility of synchronous signal detection via modulation transfer spectroscopy. Typically in modulation transfer spectroscopy one modulates just one character of the pump field, for example either amplitude or frequency but not both. For example in Ref.**??** a mechanical chopper was used on the pump beam of the SAS modulating just the laser field amplitude. Note that the 780nm transition's doppler envelope is much wider ($\sim$ 500MHz) than both the 776nm intrinsic linewidth (a few MHz for each line and a hyperfine manifold spread of $\sim$ 20 MHz) and the 776nm free running laser linewidth (not directly measured, but also typically $<$ 10 MHz on timescales of roughly 0.1 mS, consistent with our observations). This means that a measurement of the 776nm laser+atomic transition lineshape is very nearly independent of the 780nm laser's detuning.

To measure the 776nm laser+atomic transition lineshape then we chose to directly modulate the current of the 780nm laser, in confidence that only its intensity modulation (assumed to be much slower than the 5P excited state lifetime) would imprint on the atomic response to the 776nm laser. For our measurement we lightly modulated the 780nm diode at a depth of $<$ 0.1mA at about 50 KHz with the reference provided by the lockin amplifier and demodulated the 776nm laser's transmission as we slew the later's frequency at just a few Hz across the transition via a current ramp[52].

This approach had some marked advantages compared to modulation transfer example employed via SAS in Ref.[2]. No reference input to the lock-in amplifier the voltage from an additional amplified photodetector as in that example employing the chopper. Primarily due to greater modulation frequency one can also complete the data capture atleast an order of magnitude more quickly than in that reference.

The output as shown in Fig. 5 is similar to the earlier absorption traces and the direct flourescence measurement data, revealing that the free running 776nm laser is spectrally too wide and noisy to resolve individual excited state hyperfine levels, but does capture the expected the smeared density of known states in the $5D^{5/2}$.

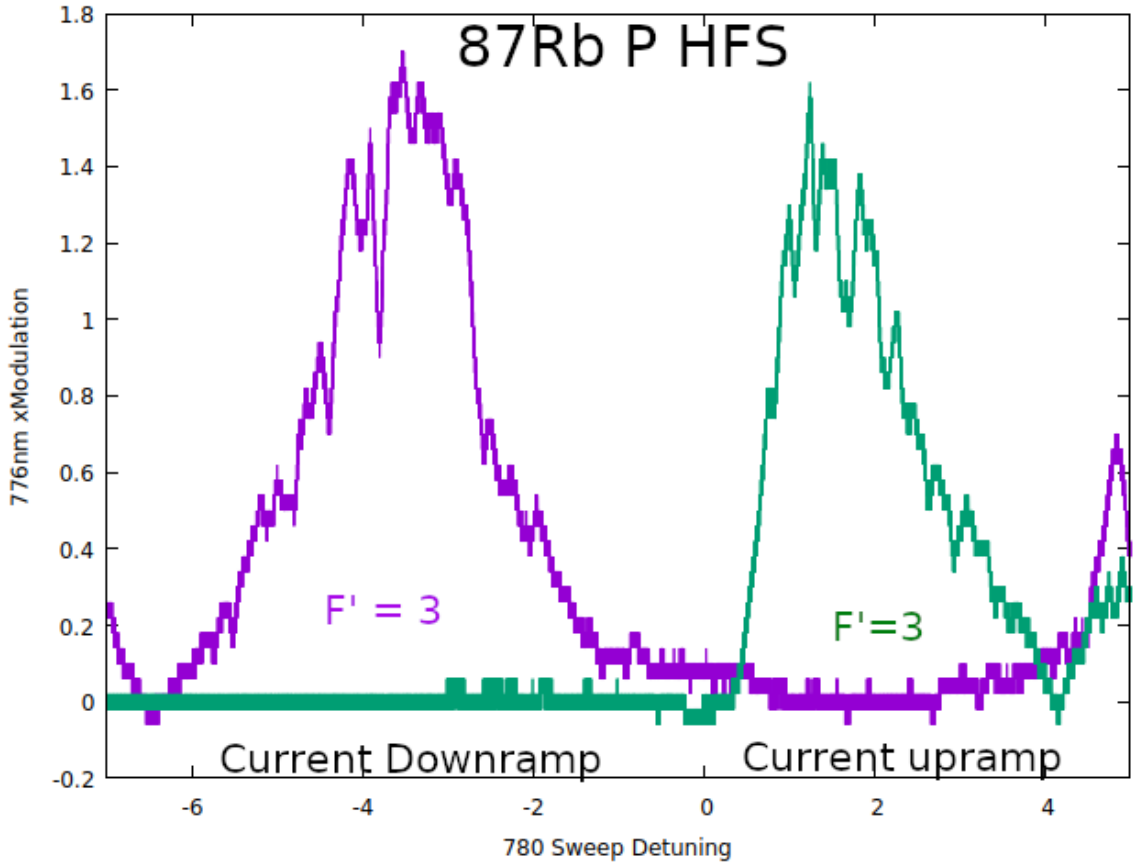

FIG. 5. Lineshape of 776nm laser on the $5D^{5/2}$ states from modulation transfer spectroscopy as described in the text.

VI. CONCLUSION

It had already been established that frequency-noisy free-running laser diodes are ideal for a straightforward, pedagogically useful and inexpensive undergraduate advanced laboratory measurements. In this note we highlighted their utility in a measurement of the isotope shift in the $5D^{5/2}$ state. In addition to refining student's microphysical 'picture' of the atom, most notably, by challenging common misconceptions about the motion of the electron in the

ground state, this isotope shift measurement indicates to students the necessity of including the somewhat more subtle SMS contribution. Finally, with very little modification the laboratory can demonstrate a basic use of modulation transfer spectroscopy

Because of its rich utility, relative setup ease and low cost, it is hoped that this study will aid the diffusion of this laboratory across additional undergraduate advanced laboratories.

ACKNOWLEDGMENTS

It is a pleasure to acknowledge insightful discussions with I. Novikova and F. Narducci regarding this work. This work was supported in part by the U.S. National Science Foundation (Grant NSF-DMR-2226956), and the Williamson Watanakunakorn Summer Science Program at YSU.

---

* aanderson05@student.ysu.edu

† teayers@student.ysu.edu

‡ sccart@student.ysu.edu

§ vtobarcorrea@student.ysu.edu

¶ aobpt.sail@gmail.com

** restipanovich@student.ysu.edu

†† dcphtn@gmail.com

[1] A. C. Melisinos and J. Napolitano, "Experiments in Modern Physics," 2nd Ed., Academic Press, ISBN-10 0124898513, pgs. 233-236 (2003).

[2] T.J. Bucci, J.P. Feigert, B. Chamberlain and A. Giovannone and M. Crescimanno, "Rubidium Isotope Shift Measurement using Noisy Lasers," Am. Jour. of Phys. **89**, 730 (2021).

[3] W. R. Johnson? What?

[4] A.J.Olsen, E.J. Carlson and S.K. Meyer, "Two photon spectroscopy of rubidium using a grating-feedback diode laser," Am. J. Phys, **74**(3), 218–223 (2006).

[5] D. W. Preston, "Doppler-free saturated absorption: Laser spectroscopy," Am. J. of Phys. **64**, 1432 (1996).

[6] G. P. Barwood, P. Gill, and W. R. C. Rowley, "Frequency Measurements on Optically Narrowed

Rb-Stabilised Laser Diodes at 780 nm and 795 nm," Appl. Phys. B, **53**(3) 142-147 (1991).

[7] G.P. Barwood and P. Gill and W.R.C. Rowley,"An Optically Narrowed Diode Laser for Rb Saturation Spectroscopy," Journal of Modern Optics, **37**(4), 749-758 (1990).

[8] J.C. Comparo, "The laser diode in atomic physics," Contemp. Phys. **26**(5), 443–447 (1985).

[9] Ming-Sheng Ko and Yi-Wei Liu, "Observation of rubidium 5 $S_{\frac{1}{2}}$ - 7 $S_{\frac{1}{2}}$ two-photon transitions with a diode laser," Opt. Lett. **29**(15). 1799 (2004).

[10] P. Grundevik, M. Gustavsson, A. Rosen and S. Svanberg, "High Resolution Laser Fluorescence Spectroscopy in the Deep Blue Spectral Region," Z. Physik A **283**,127–132 (1977).

[11] U. Gustafsson, J. Alnis and S. Svanberg, "Atomic spectroscopy with violet laser diodes," Am. J. Phys. **68**(7), 660-664 (2000).

[12] H. S. Moon , W.-K. Lee and H. S. Suh, "Hyperfine-structure-constant determination and absolute-frequency measurement of the Rb 4D$_{\frac{3}{2}}$ state," , Phys. Rev. A **79**, 062503 (2009).

[13] N. Prijapati, A.M. Akulshin, I. Novikova, "Comparison of collimated blue light generation in 85Rb atoms," arXiv:1802.07305v1.

[14] P. G. Pappas, M. M. Burns, D. D. Hinshelwood, M. S. Feld and D. E. Murnick, "Saturation spectroscopy with laser optical pumping in atomic barium," Phys. Rev. A, **21**(6) , 1955–1968 (1980).

[15] J. R. Brandenberger, "Hyperfine splittings in $4p^5$5p configuration of ^{83}Kr using saturated absorption laser spectroscopy," Phys. Rev. A **39**, 64 (1989).

[16] D. E. Roberts and E. N. Fortson, "Rubidium isotope shifts and hyperfine structure by two-photon spectroscopy with a multi-mode laser," Opt. Comm., **14**(3), 332 (1975).

[17] Y. Kato and B. P. Stoicheff, "Two-photon absorption to highly excited D states of Rb atoms, " J. Opt. Soc. Am., **66**(5), 490–492 (1976).

[18] F. Nez, F. Biraben, R. Felder and Y. Millerioux, "Optical frequency determination of the hyperfine components of the $5S_{1/2}$-$5D_{3/2}$ two-photon transitions in rubidium," Opt. Comm. **102** 432-438 (1993).

[19] C. Glaser, F. Karlewski, J. Kluge, J. Grimmel, M. Kaiser, A. Günther, H. Hattermann, M. Krutzik and J. Fortágh, "Absolute frequencey measurement of rubidium 5S-6P transitions," Phys. Rev. A. **102**, 012804 (2020).

[20] B. Ohayon, H. Rahangdale, A. J. Geddes, J. C. Berengut and G. Ron, "Isotope shifts in ^{20,22}Ne: Precision measurements and global analysis in the framework of intermediate coupling," Phys.

Rev. A, **99**, 042503 (2019).

[21] A. O. Neely, K. Cassella, S. Eustice, D. M. Stamper-Kurn, "Isotope shifts in the metastable a^5F and excited y^5G^0 terms of atomic titanium," Phys. Rev. A, **103**, 032818 (2021).

[22] C. E. Wieman and L. Hollberg, "Using diode lasers for atomic physics," Rev. Sci. Instrum. **62**(1) 1–20 (1991).

[23] D. S. Hughes and C. Eckart, "The effect of the motion of the nucleus on the spectra of LiI and LiII," Phys. Rev. **36** , 694 (1930).

[24] E. Arimondo,M. Inguscio,and P. Violino, "Experimental determination of the hyperfine structure in the alkali atoms," Rev. of Modern Physics, **49**(1), 31 (1977).

[25] A. Corney, *Atomic and Laser Spectroscopy*, Clarendon Press (Oxford) 1977, Pg. 668.

[26] A. Corney, *Atomic and Laser Spectroscopy*, Clarendon Press (Oxford) 1977, Pg. 718.

[27] R. Bruch, K. Heilig, D. Kaletta, A. Stuedel, and D. Wendlandt, "Nuclear volume and mass effect in the optical isotope shift of light elements," Journal de Physique Colloques, **30** (C1), 51-C1-58 (1969).

[28] L. Aldridge, P. L. Gould, and E. E. Eyler, "Experimental isotope shifts of the 5 $^2S_{1/2}$ state and low-lying excited states of Rb," Phys. Rev. A **84** 034501 (2011).

[29] K. Mikami, M. Tanaka, Y. Yamamoto, "Probing new intra-atomic force with isotope shifts," Eur. Phys. J. C **77** 896 (2017).

[30] Y. Yamamoto, "Probing New Intra-Atomic Force with Isotope Shifts: A Neat Thing to Do," arXiv:1810.07146v1 (2018).

[31] Julian C. Berengut, Dmitry Budker, C´edric Delaunay, Victor V. Flambaum, Claudia Frugiuele, Elina Fuchs, Christophe Grojean, Roni Harnik, Roee Ozeri, Gilad Perez, and Yotam Soreq "Probing New Long-Range Interactions by Isotope Shift Spectroscopy," Phys. Rev. Lett., **120**, 091801,(2018).

[32] H. M. Gibbs and G. C. Churchill, "Laser spectroscopic measurement of the ^{87}Rb-^{85}Rb D_1 line isotope shift," , J. Opt. Soc. Am. **62**(10), 1130 (1972).

[33] A. Banerjee, D. Das, and V. Natarajan, "Precise frequency measurements of atomic transitions by use of a Rb-stabilized resonator," Opt. Lett. **28**(17), 1579–1581 (2003).

[34] J. R. Beacham and K. L. Andrews, "Optical study of the hyperfine structure of the rubidium resonance lines," J. Opt. Soc. Am., **62**, 231 (1971).

[35] Y. Kato and B. P. Stoicheff, "Two-photon absorption to highly excited D states of Rb atoms,"

Jour. Opt. Soc. Am., **66** 490–492 (1976).

[36] B. P. Stoicheff and E. Weinberger, "Doppler-free two-photon absorption spectrum of rubidium", Can. J. Phys., **57** 2143–2154 (1979).

[37] J. C. Camparo and C. M. Klimcak, "Laser spectroscopy on a "shoestring"," Am. J. Phys. **51**, 1077 (1983).

[38] J. Blue, S. B. Bayram, and S. D. Marcum, "Creating, implementing, and sustaining an advanced optical spectroscopy laboratory course," Am. J. Phys. **78**, 503 (2010).

[39] C. Leahy, J. T. Hastings, P.M. Wilt, "Temperature dependence of Doppler broadening in rubidium:an undergraduate experiment," Am J. Phys, **65**(5) 367 (1987).

[40] A. J. Hachtel, J. D. Kleykamp, D. G. Kane, M. D. Marshall, B. W. Worth, J. T. Barkeloo, J. C. B. Kangara, J. C. Camenisch, M. C. Gillette, and S. Bali "An undergraduate measurement of radiative broadening in atomic vapor," Am. J. Phys. **80**, 740 (2012).

[41] V. Jacques, B. Hingant, A. Allafort, M. Pigeard and J. F. Roc, "Nonlinear spectroscopy of rubidium:an undergraduate experiment," Eur. J. Phys. **30** 921—934 (2009).

[42] C. H. H. Schulte, G. M. Müller, H. Horn, J. Hübner, and M. Oestreicha, "Analyzing atomic noise with a consumer sound card," Am. J. Phys. **80**, 240 (2012).

[43] B. E.Sherlock and I. G. Hughes, "How weak is a weak probe in spectroscopy?" Am. J. Phys. **77**(2) 111–115 (2009).

[44] D. A. Smith and I. G. Hughes, "The role of hyperfine pumping in multilevel systems exhibiting saturated absorption," Am. J. Phys. **72**(5), 631–637 (2004).

[45] G. N. Rao, M. N. Reddy, and E. Hecht "Hyperfine structure studies using temperature/current tuning of laser diodes: An undergraduate experiment," Am. J. Phys. **66**(8), 702 (1998).

[46] H. D. Wizeman and K. Miemax, "Isotope selective element analysis by diode laser atomic absorption spectroscopy," Mikrochim. Acta. **129** 209–216 (1998).

G. M. Tino , M. Inguscio, "Experimental indication of a nuclear volume contribution to the isotope shift in atomic oxygen," Opt. Comm. **78**(2) 158–162 (1990).

[47] A. Palffy, "Nuclear effects in atomic transitions," Contemp. Phys. **51** , 471 (2010).

[48] T. W. Hansch, I. S. Shahin, and A. L. Schawlow, "High-Resolution Saturation Spectroscopy of the Sodium D Lines with a Pulsed Tunable Dye Laser," Phys. Rev. Lett. **27**(11), 707–710 (1971).

[49] H. K. Holt, "Theory of Laser Saturation Spectroscopy," Phys. Rev. Lett. **29**(17), 1138–1140

(1972).

[50] R. Boyd, *Nonlinear Optics* (Academic Press, San Diego, 1992), Chapter 5, pp.191-239.

[51] P. N. Butcher and D. Cotter, *The Elements of Nonlinear Optics* (Cambridge U. P., Cambridge, 1990), pp. 179-188.

[52] M. Schmitt , E. A. L. Henn , J. Billy , H. Kadau , T. Maier , A. Griesmaier and T. Pfau, "Spectroscopy of a narrow-line optical pumping transition in dysprosium," Opt. Lett., **38**(5), 637–639 (2013)